Journal of Applied Mechanics and Technical Physics, Vol. 50, No. 5, pp. 792–804, 2009

SUBGRID MODELING OF FLOW PROCESSES IN AN ANISOTROPIC FRACTAL MEDIUM

O. N. Soboleva[1] and E. P. Kurochkina[2]

UDC 532.536

Equations are derived for the effective coefficients of random conductivity fields in the stationary problem of flow in an anisotropic medium. For the fields, lognormal statistics is assumed. The problem is solved using the subgrid modeling method. The results of theoretical calculations are compared with the results of direct three-dimensional numerical modeling. The results of numerical and theoretical calculations are shown to be in good agreement with each other.

Key words: *anisotropy, fractality, lognormal conductivity distribution, effective coefficients, subgrid modeling.*

Introduction. Due to sedimentation under calm conditions (in the absence of anthropogenic factors or natural catastrophes), natural inhomogeneous media take the properties of multilayered systems. It is therefore of interest to study problems of geoelectricity and filtration in anisotropic media. As a rule, the solution of such problems is based on an analytical or numerical solution of equations with piecewise constant coefficients for media with various types of regular inhomogeneities — layers. However, for media with substantial inhomogeneity, solution of the problem requires large computational efforts and is difficult to use for analysis and interpretation of results. Usually small-scale field anomalies can be taken into account by means of effective coefficients using statistical approaches [1, 2]. If the dimensions of the region in which the problem is solved are larger than the inhomogeneity scale, the effective coefficients in the region depend weakly on the formulation of the boundary problem. In this case, to determine the effective coefficients, it is necessary to take into account higher-order terms in perturbation theory [1]. This problem is solved using the field renormalization group approach [3, 4] and the subgrid modeling method [5]. In the present work, the subgrid modeling method is used to obtain equations for the effective coefficients in the problem of flow in an anisotropic medium in which the conductivity at a point is isotropic and the correlation function of the field is anisotropic. As a rule, exactly this type of anisotropy is inherent in real layers in sedimentary rock.

Formulation of the Problem. Let a local flow $\boldsymbol{v}$ and a field $\boldsymbol{h}$ be linked by the system of relations

$$\boldsymbol{v}(\boldsymbol{x}) = \sigma(\boldsymbol{x})\boldsymbol{h}(\boldsymbol{x}), \qquad \operatorname{div} \boldsymbol{v}(\boldsymbol{x}) = 0, \qquad \boldsymbol{h}(\boldsymbol{x}) = -\nabla U(\boldsymbol{x}). \tag{1}$$

In the problem of flow of a constant electric current in an inhomogeneous medium, the vector $\boldsymbol{v}$ represents the electric current density vector, the field $\boldsymbol{h}$ defined by the potential $U(\boldsymbol{x})$ is the electric field, and the local conductivity $\sigma(\boldsymbol{x})$ is the random field of the specific electrical conductivity of the medium. In the problem of filtration of a single-phase liquid in an inhomogeneous medium at small Reynolds numbers, the vector $\boldsymbol{v}$ represents the filtration velocity vector, vector $\boldsymbol{h}$ represents the field defined by the pressure gradient $[\boldsymbol{h}(\boldsymbol{x}) = -\nabla p(\boldsymbol{x})]$; the local conductivity $\sigma(\boldsymbol{x})$, equal to the ratio of the conductivity to viscosity, is the random field dependent on coordinates. The pressure and velocity are related by the Darcy equation. We assume that on the boundary Γ of the region V in which Eqs. (1) are solved, some boundary conditions are specified. The dimensions of the region V are larger than the inhomogeneity scale; therefore, the formulas for the effective coefficients in the region depend weakly on the type of boundary problem.

[1]Institute of Computational Mathematics and Mathematical Geophysics, Siberian Division, Russian Academy of Sciences, Novosibirsk 630090; olga@nmsf.sscc.ru. [2]Kutateladze Institute of Thermal Physics, Siberian Division, Russian Academy of Sciences, Novosibirsk 630090; kurochkina@itp.nsc.ru. Translated from Prikladnaya Mekhanika i Tekhnicheskaya Fizika, Vol. 50, No. 5, pp. 75–89, September–October, 2009. Original article submitted January 1, 2008; revision submitted September 4, 2008.

The field $\sigma(\boldsymbol{x})$ is modeled using the approach described in detail in [5]. The field of the physical parameter $\sigma(\boldsymbol{x})$ (conductivity, porosity, electrical conductivity, etc.) is known if it was measured with a certain step l_0. The random function of the spatial coordinates $\sigma(\boldsymbol{x})$ is treated as the limit of the parameter $\sigma_{l_0}(\boldsymbol{x})$. For $l_0 \to 0$, we have $\sigma_{l_0}(\boldsymbol{x}) \to \sigma(\boldsymbol{x})$. Similarly to [6, 7], a dimensionless field ψ equal to the ratio of the conductivities smoothed on two different scales l and l' was considered in [5]. We denote by $\sigma(\boldsymbol{x})_l$ the parameter $\sigma_{l_0}(\boldsymbol{x})$ which is smoothed on the scale l. Then, $\psi(\boldsymbol{x}, l, l') = \sigma(\boldsymbol{x})_{l'}/\sigma(\boldsymbol{x})_l$ $(l' < l)$. For $l' \to l$, we have the field $\varphi(\boldsymbol{x}, l') = (\partial\psi(\boldsymbol{x}, l', l'y)/\partial y)\Big|_{y=1}$, which defines all statistical properties of the medium. As a result, we have the equation

$$\frac{\partial \ln \sigma(\boldsymbol{x})_l}{\partial \ln l} = \varphi(\boldsymbol{x}, l). \tag{2}$$

In fact, small-scale fluctuations of the field φ can be observed only in a certain finite range of scales $l_0 < l < L$. The solution of Eq. (2) has the form

$$\sigma_{l_0}(\boldsymbol{x}) = \sigma_0 \exp\Big(-\int\limits_{l_0}^{L} \varphi(\boldsymbol{x}, l_1)\, \frac{dl_1}{l_1}\Big), \tag{3}$$

where σ_0 is a constant.

According to the theorem of sums of independent random fields [8], if a variance $\varphi(\boldsymbol{x}, l)$ at a given point is finite, then, for large values of L/l_0, the integral in (3) tends to a value that corresponds to a field with a normal probability distribution. If the variance of the field $\varphi(\boldsymbol{x}, l)$ is infinite and if a nondegenerate (not concentrated at one point) limiting distribution of the sum of random variables exists, this distribution is stable. In the present work, it is assumed that the field $\varphi(\boldsymbol{x}, l)$ has a normal distribution and a homogeneous correlation function:

$$\langle \varphi(\boldsymbol{x}, l)\, \varphi(\boldsymbol{y}, l')\rangle - \langle \varphi(\boldsymbol{x}, l)\rangle\langle \varphi(\boldsymbol{y}, l')\rangle = \Phi(\boldsymbol{x} - \boldsymbol{y}, l, l')\, \delta(\ln l - \ln l') \tag{4}$$

(the angular brackets denote statistical averaging). It is assumed that the fluctuations of the field φ in different scales do not correlate. This assumption, which is usual for scaling models, corresponds to the fact that the statistical dependence becomes insignificant if the fluctuation scales of the parameters are different in value. If the medium is self-similar, then, for any positive value of K, the following condition holds:

$$\Phi(\boldsymbol{x} - \boldsymbol{y}, l) = \Phi(K\boldsymbol{x} - K\boldsymbol{y}, Kl).$$

According to the conservative description of the cascade [7], any l should satisfy the equality $\langle \sigma_l(\boldsymbol{x})\rangle = \sigma_0$. For fields such as the porosity field, this condition follows from their physical meaning and it is also valid for conductivity fields and electrical conductivity if one assumes the ergodic hypothesis, i.e., the possibility of smoothing over large volumes equivalent to statistical averaging. Equation (3) for the conservative cascade implies that

$$\Big\langle \exp\Big(-\int\limits_{l_0}^{L} \varphi(\boldsymbol{x}, l_1)\, \frac{dl_1}{l_1}\Big)\Big\rangle = 1. \tag{5}$$

In the special case of uncorrelated fluctuations of the field φ of different scales (4), equality (5) is satisfied provided that

$$\Phi_0(l) = 2\langle \varphi(l)\rangle, \tag{6}$$

where $\Phi_0(l) = \Phi(0, l)$.

Subgrid Modeling. The conductivity function $\sigma(\boldsymbol{x}) = \sigma_{l_0}(\boldsymbol{x})$ can be divided into two components according to the scale l. The large-scale component $\sigma(\boldsymbol{x}, l)$ is obtained by statistical averaging over all $\varphi(\boldsymbol{x}, l_1)$ for $l_1 < l$, and the small-scale component is equal to $\sigma'(\boldsymbol{x}) = \sigma(\boldsymbol{x}) - \sigma(\boldsymbol{x}, l)$. Thus,

$$\begin{gathered}\sigma(\boldsymbol{x}, l) = \sigma_0 \exp\Big(-\int\limits_{l}^{L} \varphi(\boldsymbol{x}, l_1)\, \frac{dl_1}{l_1}\Big)\Big\langle \exp\Big(-\int\limits_{l_0}^{l} \varphi(\boldsymbol{x}, l_1)\, \frac{dl_1}{l_1}\Big)\Big\rangle, \\ \sigma'(\boldsymbol{x}) = \sigma(\boldsymbol{x}, l)\Big[\exp\Big(-\int\limits_{l_0}^{l} \varphi(\boldsymbol{x}, l_1)\, \frac{dl_1}{l_1}\Big) \Big/ \Big\langle \exp\Big(-\int\limits_{l_0}^{l} \varphi(\boldsymbol{x}, l_1)\, \frac{dl_1}{l_1}\Big)\Big\rangle - 1\Big].\end{gathered} \tag{7}$$

The large-scale (supergrid) component $U(\boldsymbol{x},l)$ represents the statistical mean of the solutions of system (1) in which the large-scale component $\sigma(\boldsymbol{x},l)$ is fixed and the small-scale component σ' is random, i.e., $U(\boldsymbol{x},l)=\langle U(\boldsymbol{x})\rangle$. The subgrid component is equal to $U'=U(\boldsymbol{x})-U(\boldsymbol{x},l)$. Substituting the expressions for $U(\boldsymbol{x})$ and $\sigma(\boldsymbol{x})$ into system (1) and averaging over the small-scale component, we obtain

$$\nabla[\sigma(\boldsymbol{x},l)\nabla U(\boldsymbol{x},l)+\langle\sigma'(\boldsymbol{x})\nabla U'(\boldsymbol{x})\rangle]=0. \tag{8}$$

In Eq. (8), the unknown second term cannot be rejected without tentative estimation since the correlation between the conductivity and potential gradient can be significant [1]. The choice of the form of the second term in (8) defines the subgrid model. The value of this term is estimated using perturbation theory. Let the initial value of the scale l be close to the smallest scale l_0. Taking into account (8) and ignoring second-order terms as was done in [5], from system (1) we obtain the subgrid equation

$$\Delta U'(\boldsymbol{x})=-\frac{1}{\sigma(\boldsymbol{x},l)}\,\nabla\sigma'(\boldsymbol{x})\nabla U(\boldsymbol{x},l). \tag{9}$$

Because an insignificant change in the scale $\sigma(\boldsymbol{x},l)$ causes significant fluctuations of the field (which is characteristic of fractal fields), it can be assumed that the field and its derivatives change more slowly than the quantity $\sigma'(\boldsymbol{x})$ and its derivatives. The same assumptions is made for the field $U(\boldsymbol{x},l)$. According to the subgrid modeling method, the quantities $\sigma(\boldsymbol{x},l)$ and $U(\boldsymbol{x},l)$ on the right side of Eqs. (9) are considered known. Because the values of $U'(\boldsymbol{x})$ on the boundary are equal to zero, the solution of Eq. (9) has the form

$$U'(\boldsymbol{x})=\frac{1}{4\pi\sigma(\boldsymbol{x},l)}\Big(\int\limits_V\frac{1}{r}\,\nabla'\sigma'(\boldsymbol{x}')\,d\boldsymbol{x}'\Big)\,\nabla U(\boldsymbol{x},l), \tag{10}$$

where $r=|\boldsymbol{x}-\boldsymbol{x}'|$; ∇' denotes differentiation with respect to the variable $\boldsymbol{x}'$. The quantity $\nabla U(\boldsymbol{x},l)$ is taken out of the integral, according to the assumptions adopted above. Using (10), the subgrid term in Eq. (8) is expressed as

$$\begin{aligned}\langle\sigma'(\boldsymbol{x})\nabla_i U'(\boldsymbol{x})\rangle&=\frac{1}{4\pi\sigma(\boldsymbol{x},l)}\Big\langle\sigma'(\boldsymbol{x})\int\limits_V\nabla_i\,\frac{1}{r}\,\nabla'_j\sigma'(\boldsymbol{x}')\,d\boldsymbol{x}'\Big\rangle\nabla_j U(\boldsymbol{x},l)\\&=-\frac{1}{4\pi\sigma(\boldsymbol{x},l)}\int\limits_V\nabla'_i\,\frac{1}{r}\,\nabla'_j\langle\sigma'(\boldsymbol{x})\sigma'(\boldsymbol{x}')\rangle\,d\boldsymbol{x}'\,\nabla_j U(\boldsymbol{x},l).\end{aligned} \tag{11}$$

Here $\nabla_i=\partial/\partial x_i$; the summation is performed from 1 to 3 over repeated indices. For a lognormal distribution of the conductivity probabilities, formula (7) for the statistical moments implies that, for small $dl=l-l_0$, the following equalities are valid:

$$\sigma(\boldsymbol{x},l)=\sigma_l(\boldsymbol{x})\Big(1-\langle\varphi\rangle\,\frac{dl}{l}+\frac{1}{2}\,\Phi_0(l)\,\frac{dl}{l}\Big), \tag{12}$$

$$\langle\sigma'(\boldsymbol{x})\sigma'(\boldsymbol{x}')\rangle=\sigma(\boldsymbol{x},l)^2\Big\langle\exp\Big(-\int\limits_{l_0}^{l}(\varphi(\boldsymbol{x},l_1)+\varphi(\boldsymbol{x}',l_1)-2\langle\varphi\rangle+\Phi_0(l_1))\,\frac{dl_1}{l_1}\Big)-1\Big\rangle\approx\sigma(\boldsymbol{x},l)^2\Phi(\boldsymbol{x}-\boldsymbol{x}',l)\,\frac{dl}{l}\,. \tag{13}$$

Substitution of (13) into (11) yields

$$\langle\sigma'(\boldsymbol{x})\nabla_i U'(\boldsymbol{x})\rangle=\eta_{ij}\sigma(\boldsymbol{x},l)\,\nabla_j U(\boldsymbol{x},l)\,\frac{dl}{l},\qquad\eta_{ij}=-\frac{1}{4\pi}\int\limits_V\nabla'_i\,\frac{1}{r}\,\nabla'_j\Phi(\boldsymbol{x}-\boldsymbol{x}',l)\,d\boldsymbol{x}'. \tag{14}$$

The integral over the region V in formula (14) can be replaced by the integral with infinite limits because the integrand correlation function is small if $|\boldsymbol{x}-\boldsymbol{x}'|>L$ ($L\ll L_0$, where L_0 is the smallest size of the region V and L is the largest inhomogeneity scale). With such a replacement, the error is significant only in a narrow region (whose size is equal to the correlation radius) near the boundary. To calculate integral (14), it is necessary to know the correlation function Φ. Determining the form of the correlation function from experimental data or natural measurements is difficult (see, for example, [9, 10]). To determine the degree of the effect of the form of the correlation function on the effective coefficients proposed in the present work, we compare two correlation functions and the frequently used rectangular approximation of correlation functions. The conducting medium will

be considered stratified so that the conductivity along the coordinates x_1 and , x_2 has identical inhomogeneity scales. Let, along the x_1 and x_2 axes, the scale be equal to $l_1 = \alpha_1 l$, and along the x_3 axis, to $l_2 = \alpha_2 l$ (α_1 and α_2 are positive constants). Identical scales on the two axes are considered in order to avoid lengthy calculations and numerical calculations of elliptic integrals that arise from integration of correlation functions for three-dimensional structures. Let us consider the correlation function

$$\Phi_1(\boldsymbol{x}, l) = \Phi_0(l) \exp\Big(- \frac{\alpha_1^2}{l^2} [(x_1' - x_1)^2 + (x_2' - x_2)^2] - \frac{\alpha_2^2}{l^2} (x_3' - x_3)^2 \Big). \tag{15}$$

For $i = j$ ($i = 1, 2$), $\alpha_1 < \alpha_2$, and $c^2 = (\alpha_2^2 - \alpha_1^2)/\alpha_1^2$, the integral in (14) is equal to

$$\eta_{11} = \frac{c^2 + 1}{2c^2} \Big(\frac{1}{c} \arctan c - \frac{1}{c^2 + 1} \Big).$$

For $i \neq j$, the integral is equal to zero since, in this case, the integrand function l is odd. For $i = j = 3$, the integral is equal to

$$\eta_{12} = \frac{c^2 + 1}{c^2} \Big(1 - \frac{1}{c} \arctan c \Big).$$

For $i = j$ ($i = 1, 2$), $\alpha_1 > \alpha_2$, and $c^2 = (\alpha_1^2 - \alpha_2^2)/\alpha_1^2$, the integral in (14) is equal to

$$\eta_{11} = \frac{1 - c^2}{2c^2} \Big(\frac{1}{2c} \ln \Big(\frac{1 + c}{1 - c} \Big) - \frac{1}{1 - c^2} \Big),$$

and for $i = j = 3$, the integral in (14) is equal to

$$\eta_{12} = \frac{1 - c^2}{c^2} \Big(\frac{1}{2c} \ln \Big(\frac{1 + c}{1 - c} \Big) - 1 \Big).$$

Using the obtained expressions for the integrals and formula (12) and neglecting terms of the second order in dl, we obtain the following estimate for the second term in the supergrid equation:

$$\begin{gathered} \langle \sigma'(\boldsymbol{x}) \nabla_i U'(\boldsymbol{x}) \rangle \simeq \Big(\frac{\Phi_0}{2} - \Phi_0 \eta_{11} - \langle \varphi \rangle \Big) \frac{dl}{l} \langle \sigma_l(\boldsymbol{x}) \nabla_i U(\boldsymbol{x}, l) \rangle, \qquad i = 1, 2, \\ \langle \sigma'(\boldsymbol{x}) \nabla_3 U'(\boldsymbol{x}) \rangle \simeq \Big(\frac{\Phi_0}{2} - \Phi_0 \eta_{12} - \langle \varphi \rangle \Big) \frac{dl}{l} \langle \sigma_l(\boldsymbol{x}) \nabla_3 U(\boldsymbol{x}, l) \rangle. \end{gathered} \tag{16}$$

Substituting (16) into (8) and letting dl to zero, we obtain the following equations for the effective local flow:

$$\frac{d \ln \sigma_{0l}^1}{d \ln l} = \frac{\Phi_0}{2} - \Phi_0 \eta_{11} - \langle \varphi \rangle, \qquad \frac{d \ln \sigma_{0l}^2}{d \ln l} = \frac{\Phi_0}{2} - \Phi_0 \eta_{12} - \langle \varphi \rangle. \tag{17}$$

For $\alpha_2 \to \alpha_1$, the result corresponds to the isotropic case: $\eta_{11} = \eta_{12} = 0.333$. In the estimation, the scale invariance property can be ignored. This implies that the coefficients α_1 and α_2 can also be scale functions. If the medium is scale invariant, the solution of Eqs. (17) has the form

$$\sigma_{0l}^1 = \sigma_{0L} (l/L)^{\Phi_0/2 - \Phi_0 \eta_{11} - \langle \varphi \rangle}, \qquad \sigma_{0l}^2 = \sigma_{0L} (l/L)^{\Phi_0/2 - \Phi_0 \eta_{12} - \langle \varphi \rangle}. \tag{18}$$

Let us consider the second anisotropic correlation function of conductivity [10]:

$$\Phi_2(\boldsymbol{x}, l) = \Phi_0 \exp\Big(- \frac{\alpha_1}{l} \sqrt{(x_1' - x_1)^2 + (x_2' - x_2)^2} - \frac{\alpha_2}{l} |x_3' - x_3| \Big). \tag{19}$$

For the function (19), the integral in (14) is equal to

$$\eta_{21} = \frac{\sqrt{c^2 - 1}}{4c^3} \Big(2 \ln \Big(c + \sqrt{c^2 - 1} \Big) + \ln \frac{c + 1}{c - 1} \Big) - \frac{\sqrt{c^2 - 1} \, (1 - \sqrt{c^2 - 1})}{2c^2},$$

$$\eta_{22} = - \frac{\sqrt{c^2 - 1}}{2c^3} \Big(2 \ln \Big(c + \sqrt{c^2 - 1} \Big) + \ln \frac{c + 1}{c - 1} \Big) + \frac{1 + \sqrt{c^2 - 1}}{c^2}.$$

TABLE 1

Parameters η_{ij} versus Ratio α_1/α_2

α_1/α_2	η_{11}/η_{12}	η_{21}/η_{22}	η_{31}/η_{32}
0.01	0.008/0.985	0.022/0.957	0.005/0.991
0.05	0.037/0.926	0.070/0.861	0.023/0.955
0.25	0.148/0.704	0.179/0.642	0.110/0.781
0.50	0.236/0.527	0.244/0.511	0.205/0.590
1.00	0.333/0.333	0.312/0.377	0.333/0.333
5.00	0.472/0.056	0.432/0.136	0.488/0.025
10.00	0.490/0.020	0.461/0.078	0.497/0.006
20.00	0.497/0.007	0.479/0.043	0.499/0.002

Here $c^2 = (\alpha_1^2 + \alpha_2^2)/\alpha_2^2$. As $\alpha_2 \to \alpha_1$, we have $\eta_{21} = 0.312$ and $\eta_{22} = 0.377$, i.e., the anisotropy is preserved. Because it is difficult to determine the form of the correlation function from experimental data, in some cases, the correlation function [1] is approximated as

$$\Phi_3(\boldsymbol{x}, l) = \begin{cases} \Phi_0, & |x_i| \le l/\alpha_i,\ i = 1, \ldots, 3, \\ 0, & |x_i| > l/\alpha_i. \end{cases} \tag{20}$$

The function Φ_3 may not always be used to approximate the correlation function because, for some frequency values, its spectral density takes negative values. The function $\Phi_3(\boldsymbol{x}, l)$ is not isotropic because if all coefficients α_i are identical, the parallelepiped becomes a cube. For the approximation (20), we calculate the integral in (14):

$$\eta_{31} = \frac{2}{\pi} \arctan \frac{\alpha_1}{\sqrt{2\alpha_2^2 + \alpha_1^2}}, \qquad \eta_{32} = \frac{2}{\pi} \arctan \frac{\alpha_2^2}{\alpha_1 \sqrt{2\alpha_2^2 + \alpha_1^2}}.$$

For $\alpha_1 = \alpha_2$, we have $\eta_{31} = \eta_{32} = 0.333$. Thus, we obtain the result which corresponds to the isotropic case, although the employed function is anisotropic. The values of the parameters η_{ij} calculated as functions of the ratio α_1/α_2, indicate that the mean local flow depends insignificantly on the form of the correlation function (Table 1). From Table 1, it follows that the results of calculations using all functions Φ_i are close except in the region in which the values of η_{ij} are small. However, for this region, the corrections in estimating the mean local flow are negligibly small. Thus, the effective coefficients depend mainly on the scale of correlations on various coordinate axes.

Let us determine the effective coefficients for estimating the tensor of the second statistical one-point moments of the field $\boldsymbol{h}$. At the point $\boldsymbol{x}$, the tensor components of the second statistical moment are equal to

$$\langle h_n(\boldsymbol{x}) h_j(\boldsymbol{x}) \rangle = \nabla_n U(\boldsymbol{x}, l)\, \nabla_j U(\boldsymbol{x}, l) + \langle \nabla_n U'(\boldsymbol{x})\, \nabla_j U'(\boldsymbol{x}) \rangle. \tag{21}$$

Let us estimate the second term in (21). We denote $r_1 = |\boldsymbol{x} - \boldsymbol{x}'|$ and $r_2 = |\boldsymbol{x} - \boldsymbol{x}''|$. Using formula (9), we obtain the correlation tensor components for $\nabla U'$:

$$\begin{gathered} \langle \nabla_n U'(\boldsymbol{x})\, \nabla_j U'(\boldsymbol{x}) \rangle = I\, \nabla_m U(\boldsymbol{x}, l)\, \nabla_k U(\boldsymbol{x}, l)\, \frac{dl}{l}, \\ I = \frac{1}{16\pi^2} \iint \nabla'_n \frac{1}{r_1} \nabla''_j \frac{1}{r_2}\, \nabla'_m\, \nabla''_k \Phi(\boldsymbol{x}'' - \boldsymbol{x}', l)\, d\boldsymbol{x}''\, d\boldsymbol{x}'. \end{gathered} \tag{22}$$

Calculating the integral in (22) for $n = j$ using the correlation function (15), for the second statistical moment of the field $\boldsymbol{h}(\boldsymbol{x})$ we obtain

$$\begin{bmatrix} \langle h_1(\boldsymbol{x})^2 \rangle \\ \langle h_2(\boldsymbol{x})^2 \rangle \\ \langle h_3(\boldsymbol{x})^2 \rangle \end{bmatrix} = \begin{bmatrix} h_1(\boldsymbol{x}, l)^2 \\ h_2(\boldsymbol{x}, l)^2 \\ h_3(\boldsymbol{x}, l)^2 \end{bmatrix} + \Phi_0(l)\, \frac{dl}{l}\, A_1 \begin{bmatrix} h_1(\boldsymbol{x}, l)^2 \\ h_2(\boldsymbol{x}, l)^2 \\ h_3(\boldsymbol{x}, l)^2 \end{bmatrix}, \tag{23}$$

where the matrix A_1 for $\alpha_1 < \alpha_2$, $c^2 = (\alpha_2^2 - \alpha_1^2)/\alpha_1^2$, and $b = \arctan c$ is equal to

$$A_1 = \begin{bmatrix} \dfrac{3(c^2-3)(c^2+1)}{16c^5}\, b + \dfrac{3(c^2+3)}{16c^4} & \dfrac{(c^2-3)(c^2+1)}{16c^5}\, b + \dfrac{c^2+3}{16c^4} & \dfrac{(c^2+3)(c^2+1)}{4c^5}\, b - \dfrac{3(1+c^2)}{4c^4} \\ \dfrac{(c^2-3)(c^2+1)}{16c^5}\, b + \dfrac{c^2+3}{16c^4} & \dfrac{3(c^2-3)(c^2+1)}{16c^5}\, b + \dfrac{3(c^2+3)}{16c^4} & \dfrac{(c^2+3)(c^2+1)}{4c^5}\, b - \dfrac{3(1+c^2)}{4c^4} \\ \dfrac{(c^2+3)(c^2+1)}{4c^5}\, b - \dfrac{3(1+c^2)}{4c^4} & \dfrac{(c^2+3)(c^2+1)}{4c^5}\, b - \dfrac{3(1+c^2)}{4c^4} & -\dfrac{3(c^2+1)^2}{2c^5}\, b + \dfrac{(c^2+1)(2c^2+3)}{2c^4} \end{bmatrix},$$

and for $\alpha_1 > \alpha_2$, $c^2 = (\alpha_1^2 - \alpha_2^2)/\alpha_1^2$, and $b = \ln((1+c)/(1-c))$, we have

$$A_1 = \begin{bmatrix} -\dfrac{3(1-c^2)(c^2+3)}{32c^5}\,b - \dfrac{3(c^2-3)}{16c^4} & -\dfrac{(1-c^2)(c^2+3)}{32c^5}\,b - \dfrac{c^2-3}{16c^4} & \dfrac{(1-c^2)(3-c^2)}{8c^5}\,b - \dfrac{3(1-c^2)}{4c^4} \\ -\dfrac{(1-c^2)(c^2+3)}{32c^5}\,b - \dfrac{c^2-3}{16c^4} & -\dfrac{3(1-c^2)(c^2+3)}{32c^5}\,b - \dfrac{3(c^2-3)}{16c^4} & \dfrac{(1-c^2)(3-c^2)}{8c^5}\,b - \dfrac{3(1-c^2)}{4c^4} \\ \dfrac{(1-c^2)(3-c^2)}{8c^5}\,b - \dfrac{3(1-c^2)}{4c^4} & \dfrac{(1-c^2)(3-c^2)}{8c^5}\,b - \dfrac{3(1-c^2)}{4c^4} & -\dfrac{3(1-c^2)^2}{4c^5}\,b - \dfrac{(1-c^2)(2c^2-3)}{2c^4} \end{bmatrix}.$$

The matrix A_1 is symmetric; therefore, it has real eigenvalues λ_i and independent eigenvectors. In Eq. (23), we make the change of variables $u_i(\boldsymbol{x}, l) = Th_i^2(\boldsymbol{x}, l)$ (T is a transformation that reduces the matrix A_1 to diagonal form). As in the estimation of the mean local flow, taking into account relation (12), we obtain the equation

$$\frac{d\ln\hat{\sigma}_l^i}{d\ln l} = \Phi_0 + \lambda_i\Phi_0 - 2\langle\varphi\rangle.$$

Hence, for a scale-invariant medium, the vector components $u_i(\boldsymbol{x}, l)$ are calculated by the formula

$$u_i(\boldsymbol{x}) = (l/L)^{\Phi_0+\lambda_i\Phi_0-2\langle\varphi\rangle}u_i(\boldsymbol{x}, l).$$

Applying the inverse transformation $\boldsymbol{u}$ to the vector T^{-1}, we obtain the estimate for $\langle h(\boldsymbol{x})^2\rangle$.

Let us estimate the quantity $\langle h_n(\boldsymbol{x})h_j(\boldsymbol{x})\rangle$ using the correlation function Φ_1, if $n \neq j$. For $\alpha_1 < \alpha_2$, the integral in (22) is equal to

$$\eta_{112} = \frac{c^2+3}{8c^4} + \frac{(c^2-3)(c^2+1)}{8c^5}\arctan c, \quad \eta_{113} = -\frac{3(c^2+1)}{4c^4} + \frac{(c^2+1)(3+c^2)}{4c^5}\arctan c,$$

and for $\alpha_1 > \alpha_2$,

$$\eta_{112} = \frac{3-c^2}{16c^4} - \frac{(1-c^2)(c^2+3)}{32c^5}\ln\Big(\frac{1+c}{1-c}\Big), \quad \eta_{113} = \frac{(3-c^2)(1-c^2)}{8c^5}\ln\Big(\frac{1+c}{1-c}\Big) - \frac{3(1-c^2)}{4c^4}$$

($\eta_{123} = \eta_{113}$). For $n \neq j$, the effective coefficients for the tensor elements of the second statistical moment of the vector $\boldsymbol{h}(\boldsymbol{x})$ are given by

$$\frac{d\ln\hat{\sigma}_l^1}{d\ln l} = \Phi_0 + \eta_{112}\Phi_0 - 2\langle\varphi\rangle, \qquad \frac{d\ln\hat{\sigma}_l^2}{d\ln l} = \Phi_0 + \eta_{113}\Phi_0 - 2\langle\varphi\rangle.$$

For a scale-invariant medium, the estimates of the tensor elements of the second statistical moment of the vector $\boldsymbol{h}(\boldsymbol{x})$ are power-law functions of the scale

$$\langle h_1(\boldsymbol{x})h_2(\boldsymbol{x})\rangle \sim (l/L)^{\Phi_0+\eta_{112}\Phi_0-2\langle\varphi\rangle}h_1(\boldsymbol{x}, l)h_2(\boldsymbol{x}, l),$$

$$\langle h_1(\boldsymbol{x})h_3(\boldsymbol{x})\rangle = \langle h_2(\boldsymbol{x})h_3(\boldsymbol{x})\rangle \sim (l/L)^{\Phi_0+\eta_{113}\Phi_0-2\langle\varphi\rangle}h_2(\boldsymbol{x}, l)h_3(\boldsymbol{x}, l).$$

If the correlation function $\Phi(\boldsymbol{x} - \boldsymbol{x}', l)$ is approximated by function (20), then in Eq. (23) for the tensor components of the second statistical moment of the vector $\boldsymbol{h}$ for $n = j$, the matrix is equal to

$$A_2 = \begin{bmatrix} -\dfrac{3c^2-2}{2\pi c^2\sqrt{2c^2-1}} + \dfrac{2}{\pi}\,b & \dfrac{1}{2\pi\sqrt{2c^2-1}} & \dfrac{c^2-1}{\pi c^2\sqrt{2c^2-1}} \\ \dfrac{1}{2\pi\sqrt{2c^2-1}} & -\dfrac{3c^2-2}{2\pi c^2\sqrt{2c^2-1}} + \dfrac{2}{\pi}\,b & \dfrac{c^2-1}{\pi c^2\sqrt{2c^2-1}} \\ \dfrac{c^2-1}{\pi c^2\sqrt{2c^2-1}} & \dfrac{c^2-1}{\pi c^2\sqrt{2c^2-1}} & -\dfrac{2(c^2-1)}{\pi c^2\sqrt{2c^2-1}} + \dfrac{2}{\pi}\,b \end{bmatrix}.$$

Here $b = \arctan\,(1/\sqrt{2c^2-1}\,)$ and $c^2 = (\alpha_1^2 + \alpha_2^2)/\alpha_1^2$. For $\alpha_1 = \alpha_2$, the matrix elements on the main diagonal are equal to 0.15, and the off-diagonal elements are equal to $9.2 \cdot 10^{-2}$. For the tensor invariant $\sum\limits_{i=1}^{3}\langle h_i(\boldsymbol{x})^2\rangle$, we obtain the same formula as for the isotropic field:

$$\sum_{i=1}^{3}\langle h_i(\boldsymbol{x})^2\rangle \approx \Big(1 + \Phi_0\,\frac{dl}{3l}\Big)\sum_{i=1}^{3}h_i(\boldsymbol{x}, l)^2.$$

TABLE 2

Elements of Matrices A_1, and A_2 versus Ratio α_1/α_2

α_1/α_2	$a_{11}/\hat{a}_{11}$	$a_{12}/\hat{a}_{12}$	$a_{13}/\hat{a}_{13}$	$a_{33}/\hat{a}_{33}$
0.01	0.003/0.001	0.001/0.001	0.004/0.002	0.977/0.986
0.05	0.015/0.006	0.005/0.006	0.017/0.011	0.891/0.933
0.25	0.069/0.029	0.023/0.027	0.056/0.052	0.592/0.676
0.50	0.125/0.067	0.042/0.053	0.070/0.084	0.387/0.421
1.00	0.200/0.150	0,066/0.092	0.066/0.092	0.200/0.150
5.00	0.340/0.323	0.113/0.153	0.019/0.012	0.017/0.001
10.00	0.362/0.336	0.121/0.157	0,008/0.003	0.005/0
20.00	0.370/0.340	0.123/0.159	0.003/0.001	0.001/0

Although the tensor invariant did not change, the diagonal elements of the matrix A_2 decreased by a factor of approximately 1.3 due to an increase in the off-diagonal elements. The weak anisotropy of the correlation function Φ_3 leads to some smoothing of the variance of the vector components $\boldsymbol{h}$. For $i \neq j$, for the tensor elements we have

$$\langle h_1(\boldsymbol{x})h_2(\boldsymbol{x})\rangle \approx \Big(1 + \frac{1}{2\pi\sqrt{2c^2-1}}\,\Phi_0\,\frac{dl}{l}\Big)h_1(\boldsymbol{x},l)h_2(\boldsymbol{x},l),$$

$$\langle h_1(\boldsymbol{x})h_3(\boldsymbol{x})\rangle \approx \Big(1 + \frac{c^2-1}{2\pi c^2\sqrt{2c^2-1}}\,\Phi_0\,\frac{dl}{l}\Big)h_1(\boldsymbol{x},l)h_3(\boldsymbol{x},l).$$

Hence,

$$\frac{d\ln\hat{\sigma}_l^1}{d\ln l} = \Big(1 + \frac{1}{2\pi\sqrt{2c^2-1}}\Big)\Phi_0 - 2\langle\varphi\rangle, \qquad \frac{d\ln\hat{\sigma}_l^2}{d\ln l} = \Big(1 + \frac{c^2-1}{2\pi c^2\sqrt{2c^2-1}}\Big)\Phi_0 - 2\langle\varphi\rangle.$$

Table 2 gives the elements of the matrices $A_1(a_{11}, a_{12}, a_{13}, a_{33})$ and $A_2(\hat{a}_{11}, \hat{a}_{12}, \hat{a}_{13}, \hat{a}_{33})$ versus the ratio α_1/α_2.

Let us estimate the correlation tensor of the local flow $\boldsymbol{v}$. The one-point second statistical moment of the local flow is equal to

$$\begin{aligned}\langle v_i(\boldsymbol{x})v_k(\boldsymbol{x})\rangle &= \sigma(\boldsymbol{x},l)^2\nabla_i U(\boldsymbol{x},l)\nabla_k U(\boldsymbol{x},l) + \sigma(\boldsymbol{x},l)^2\langle\nabla_k U'(\boldsymbol{x})\nabla_i U'(\boldsymbol{x})\rangle\\ &+ \langle\sigma'(\boldsymbol{x})^2\rangle\nabla_k U(\boldsymbol{x},l)\,\nabla_i U(\boldsymbol{x},l) + 2\langle\sigma'(\boldsymbol{x})\nabla_k U'(\boldsymbol{x})\rangle v_i(\boldsymbol{x},l) + 2\nabla_k U(\boldsymbol{x},l)\langle\sigma'(\boldsymbol{x})\nabla_i U'(\boldsymbol{x})\rangle\\ &+ \langle\sigma'(\boldsymbol{x})^2\nabla_i U'(\boldsymbol{x})\,\nabla_k U'(\boldsymbol{x})\rangle + 2\sigma(\boldsymbol{x},l)\langle\sigma'(\boldsymbol{x})\nabla_k U'(\boldsymbol{x})\nabla_i U'(\boldsymbol{x})\rangle\\ &+ \langle\sigma'(\boldsymbol{x})^2\nabla_k U'(\boldsymbol{x})\rangle\nabla_i U(\boldsymbol{x},l) + \langle\sigma'(\boldsymbol{x})^2\nabla_i U'(\boldsymbol{x})\rangle\nabla_k U(\boldsymbol{x},l). \qquad (24)\end{aligned}$$

An estimate of the second term in (24) follows from the above estimate of the second moment $\boldsymbol{h}$, an estimate of the third term follows from formulas (12) and (13), and an estimate of the fourth and fifth terms can be obtained by calculating the integral in (14). The other terms are equal to zero up to second-order terms in dl. Using (13), (16), (22), and (24), for the tensor components for $i \neq j$ and the correlation function (15), we obtain

$$\begin{bmatrix}\langle v_1(\boldsymbol{x})^2\rangle\\ \langle v_2(\boldsymbol{x})^2\rangle\\ \langle v_3(\boldsymbol{x})^2\rangle\end{bmatrix} = \begin{bmatrix}v_1(\boldsymbol{x},l)^2\\ v_2(\boldsymbol{x},l)^2\\ v_3(\boldsymbol{x},l)^2\end{bmatrix} + \Phi_0(l)\,\frac{dl}{l}\,A_3\begin{bmatrix}v_1(\boldsymbol{x},l)^2\\ v_2(\boldsymbol{x},l)^2\\ v_3(\boldsymbol{x},l)^2\end{bmatrix}.$$

For $\alpha_1 < \alpha_2$, the matrix A_3 is equal to

$$A_3 = \begin{bmatrix} -\dfrac{(29c^2+9)(c^2+1)}{16c^5}\,b + \dfrac{w}{16c^4} & \dfrac{(c^2-3)(c^2+1)}{16c^5}\,b + \dfrac{c^2+3}{16c^4} & \dfrac{(c^2+3)(c^2+1)}{4c^5}\,b - \dfrac{3(1+c^2)}{4c^4}\\ \dfrac{(c^2-3)(c^2+1)}{16c^5}\,b + \dfrac{c^2+3}{16c^4} & -\dfrac{(29c^2+9)(c^2+1)}{16c^5}\,b + \dfrac{w}{16c^4} & \dfrac{(c^2-3)(c^2+1)}{4c^5}\,b - \dfrac{3(1+c^2)}{4c^4}\\ \dfrac{(c^2-3)(c^2+1)}{4c^5}\,b - \dfrac{3(1+c^2)}{4c^4} & \dfrac{(c^2-3)(c^2+1)}{4c^5}\,b - \dfrac{3(1+c^2)}{4c^4} & \dfrac{(c^2+1)(5c^2-3)}{2c^5}\,b - \dfrac{w_1}{2c^4}\end{bmatrix}.$$

Here $b = \arctan c$, $w = 16c^4 + 35c^2 + 9$, and $w_1 = 4c^4 + 3c^2 - 3$.

For $\alpha_1 > \alpha_2$,

$$A_3 = \begin{bmatrix} \frac{(29c^2-9)(1-c^2)}{32c^5}\,b + \frac{w}{16c^4} & -\frac{(c^2+3)(1-c^2)}{32c^5}\,b - \frac{c^2-3}{16c^4} & -\frac{(c^2-3)(1-c^2)}{8c^5}\,b - \frac{3(1-c^2)}{4c^4} \\ -\frac{(c^2+3)(1-c^2)}{32c^5}\,b - \frac{c^2-3}{16c^4} & \frac{(29c^2-9)(1-c^2)}{32c^5}\,b + \frac{w}{16c^4} & -\frac{(c^2-3)(1-c^2)}{8c^5}\,b - \frac{3(1-c^2)}{4c^4} \\ -\frac{(c^2-3)(1-c^2)}{8c^5}\,b - \frac{3(1-c^2)}{4c^4} & -\frac{(c^2-3)(1-c^2)}{8c^5}\,b - \frac{3(1-c^2)}{4c^4} & -\frac{(1-c^2)(5c^2+3)}{4c^5}\,b - \frac{w_1}{2c^4} \end{bmatrix}.$$

Here $b = \ln\left((1+c)/(1-c)\right)$, $w = 16c^4 - 35c^2 + 9$, and $w_1 = 4c^4 - 3c^2 - 3$.

Next, we use the same approach as for the estimation of the second statistical moment of the vector $\boldsymbol{h}$. The matrix A_3 is reduced to diagonal form. For a scale-invariant medium, the effective coefficient for linear combinations $u_m = t_{mk} v_k(\boldsymbol{x})^2$ are power-law functions of the scale (t_{mk} are the elements of the matrix formed of the eigenvectors of the matrix A_3). In this case, the exponents depend on the eigenvalues λ_m of the matrices A_3. Applying the inverse linear transformation to the vectors u_m, we obtain an estimate for $\langle v_k(\boldsymbol{x})^2\rangle$. From (13), (16), (22), and (24), it follows that, for $i \neq j$, the correlation tensor components calculated using the correlation function (15) are equal to

$$\begin{aligned} \langle v_1(\boldsymbol{x}) v_2(\boldsymbol{x})\rangle &= \Big(1 + \Phi_0(\eta_{112} + 1 - 4\eta_{11})\,\frac{dl}{l}\Big) v_1(\boldsymbol{x}, l) v_2(\boldsymbol{x}, l), \\ \langle v_1(\boldsymbol{x}) v_3(\boldsymbol{x})\rangle &= \Big(1 + \Phi_0(\eta_{113} + 1 - 4\eta_{12})\,\frac{dl}{l}\Big) v_1(\boldsymbol{x}, l) v_3(\boldsymbol{x}, l). \end{aligned} \tag{25}$$

For $dl \to 0$, from (25) it follows that the effective coefficients satisfy the equations

$$\frac{d\ln(\hat\sigma^1_{0l})^2}{d\ln l} = 2\Phi_0 + \eta_{112}\Phi_0 - 4\eta_{11}\Phi_0 - 2\langle\varphi\rangle,$$

$$\frac{d\ln(\hat\sigma^2_{0l})^2}{d\ln l} = 2\Phi_0 + \eta_{113}\Phi_0 + 4\eta_{12}\Phi_0 - 2\langle\varphi\rangle.$$

Numerical Modeling. To verify the above formulas, as in the isotropic case, we solve the problem for a unit cube with a unit jump of the potential for $\sigma_0 = 1$. The calculations are performed for two types of boundary conditions:

1. On the cube faces $y = 0$ and $y = L_0$, the constant potential is specified: $U(x, y, z)|_{y=0} = U_1$ and $U(x, y, z)|_{y=L_0} = U_2$ ($U_1 > U_2$). The potential on the other faces of the cube is given as a linear function of y: $U = U_1 + (U_2 - U_2)y/L_0$. In this case, the largest component of the local flow is directed along the y axis, and the mean values of the components v_x and v_z are equal to zero.

2. On the cube faces $z = 0$ and $z = L_0$, a constant potential is specified, and on the other faces, the potential is given as linear function of z: $U = U_1 + (U_2 - U_2)z/L_0$. The local-flow component along the z axes is the largest, and the mean values of the components v_x and v_y are equal to zero.

The calculations are performed using dimensionless variables and a $256 \times 256 \times 256$ grid on the spatial variables. The conductivity field is modeled by formula (3), which is replaced by the finite-difference analog

$$\sigma(\boldsymbol{x})_l = \exp\Big(-\ln 2 \int\limits_{\log_2 l}^{\log_2 L} \varphi(\boldsymbol{x}, \tau)\,d\tau\Big) \approx 2^{-\sum\limits_{i=-8}^{0} \varphi(\boldsymbol{x}, \tau_i)\Delta\tau}. \tag{26}$$

Here $\tau = \log_2 l$ and $\tau_i = \log_2 l_i$ (the logarithm to base 2 is introduced for convenience); the scale step is $\Delta\tau = 1$. In the calculations, three scales were used: $\tau_1 = -6$, $\tau_2 = -5$, and $\tau_3 = -4$. The first two and the last three terms in the sum in (26) are equal to zero. Numerical modeling is performed using the algorithm by rows and columns described in [11]. A scale-invariant correlation function of a normal random field is used:

$$\Phi_1^*(\boldsymbol{x} - \boldsymbol{y}, \tau_j) = \frac{\Phi_0}{\ln 2} \exp\Big(-\frac{\alpha_1^2(x_1 - y_1)^2 + \alpha_1^2(x_2 - y_2)^2 + \alpha_2^2(x_3 - y_3)^2}{2^{2\tau_j}}\Big). \tag{27}$$

Two models of the medium are considered: 1) the inhomogeneity scales are assumed to be large on the x and y axes and small on the z axis; $\alpha_1/\alpha_2 = 0.25$; 2) the inhomogeneity scales are assumed to be small on the x

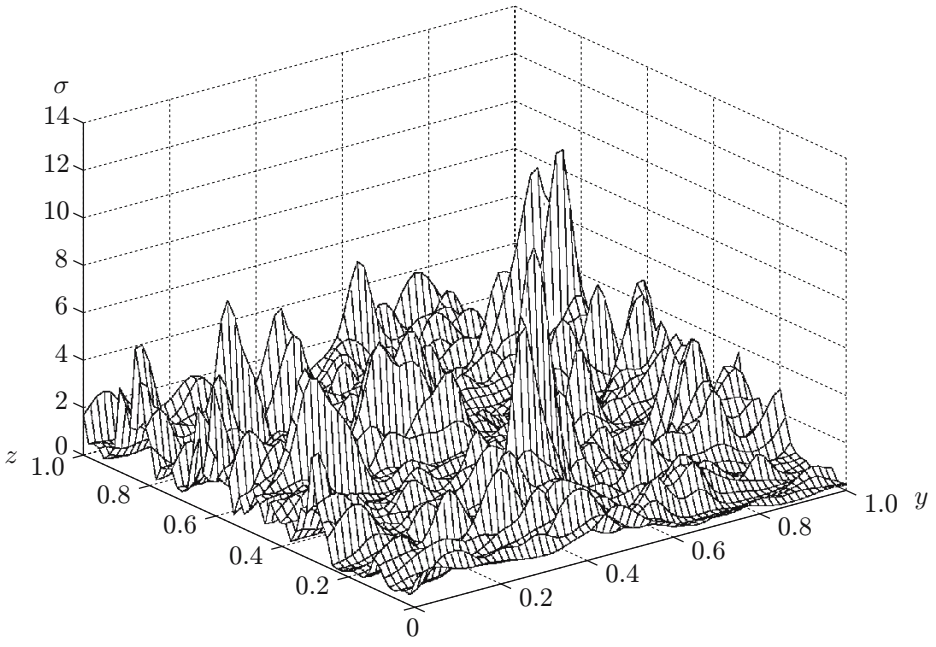

Fig. 1. Conductivity field σ [numerical modeling by formula (26)] for three scales in the midsection ($x = 0.5$, $\Phi_0 = 0.3$, $\langle\varphi\rangle = 0.15$, and $\alpha_1/\alpha_2 = 0.25$).

and y axes and large on the z axis; $\alpha_1/\alpha_2 = 4$. All results were obtained for values of the parameters $\Phi_0 = 0.3$ and $\langle\varphi\rangle = 0.15$, i.e., the conservative cascade (6) is considered. Figure 1 gives the results of numerical modeling of an anisotropic field by formula (26) (the first model of the medium).

The numerically calculated mean local flow $\boldsymbol{v}$ in the range of scales (l, L) is compared with the mean flow obtained by theoretical formulas for the same range of scales; in this case, $l \to l_0$. The effective conductivity should give the true mean local flow in the range (L, l). Since the conductivity (26) is scale-invariant, thee mean local flows are power-law functions of the scale. In fact, the exponents in formula (18) are checked. The dependences of the logarithms of the mean values of the local-flow components on the truncation scale are given to check the accuracy of the effective coefficients (18). Numerical calculations showed that, to replace statistical averaging by averaging over the space for $\alpha_1/\alpha_2 = 0.25$ and $\alpha_1/\alpha_2 = 4$, the size of the cube is insufficiently large (in both cases, the maximum scale is 1/4); therefore, additional averaging over the Gibbs ensemble was used. The generation of the coefficient and the solution of the problem was performed 80 times with the subsequent averaging over space. For the chosen parameters of the problem, this was sufficient. System (1) was solved numerically using an iterative method. In Figs. 2–7, the abscissas show the number of terms k in the sum in the exponent in formulas (26) (i.e., the number of scales used for modeling σ). Figure 2–7 give the results for the isotropic case to compare the mean local flows and the second statistical moments in the isotropic and anisotropic cases.

Figure 2 and 3 give curves of the logarithm of the mean values of the local-flow components versus the number of scales for the first and the second models of the medium. A decrease in the local flow with increasing number of scales in the medium is explained by an increase in the contact surface area between the regions with different conductivities, resulting in an increase in the flow resistance. The variance of the local flow and the field $\boldsymbol{h}$ increase for the same reason. For both models with different flow directions, the results of numerical and theoretical calculations are in good agreement. For the flow versions corresponding to Fig. 2a and Fig. 3b, the error of the estimated mean local flow for three scales does not exceed 1%, and for the flow versions corresponding to Fig. 3a and Fig. 2b, it does not exceed 8.8 and 4.2% respectively.

Figures 4 and 5 give curves of the correlation tensor of the field $\boldsymbol{h}$ versus the number of scales taken into account in the first and second models of the medium. The quantities $\langle h_x(\boldsymbol{x})^2\rangle - \langle h_x(\boldsymbol{x})\rangle^2$, $\langle h_y(\boldsymbol{x})^2\rangle - \langle h_y(\boldsymbol{x})\rangle^2$, and $\langle h_z(\boldsymbol{x})^2\rangle - \langle h_z(\boldsymbol{x})\rangle^2$ are denoted by D_x, D_y, and D_z, respectively. Figure 4a shows only two components D_x and D_y. In this case, $D_z \approx D_x$. Figure 5 shows the components D_x and D_z ($D_y = D_x$, and Fig. 5b shows $D_z \approx D_x$

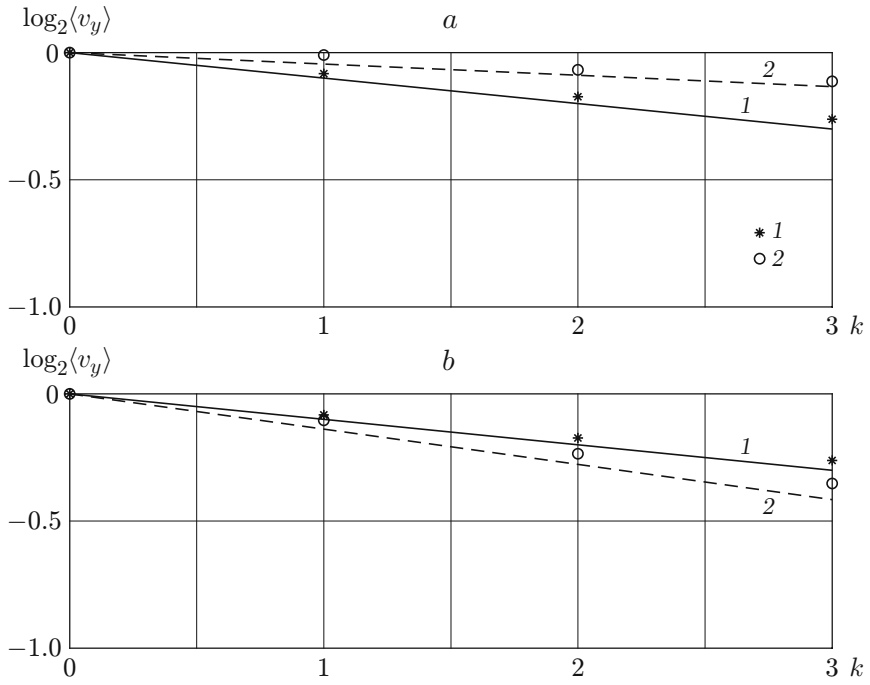

Fig. 2. Dependences of $\log_2\langle v_y\rangle$ on the number of scales (the main flow is directed along the y axis) for $\alpha_1/\alpha_2 = 0.25$ (a) and 4 (b); the curves and points show the theoretical and numerical calculations, respectively, for isotropic medium (1) and anisotropic medium (2).

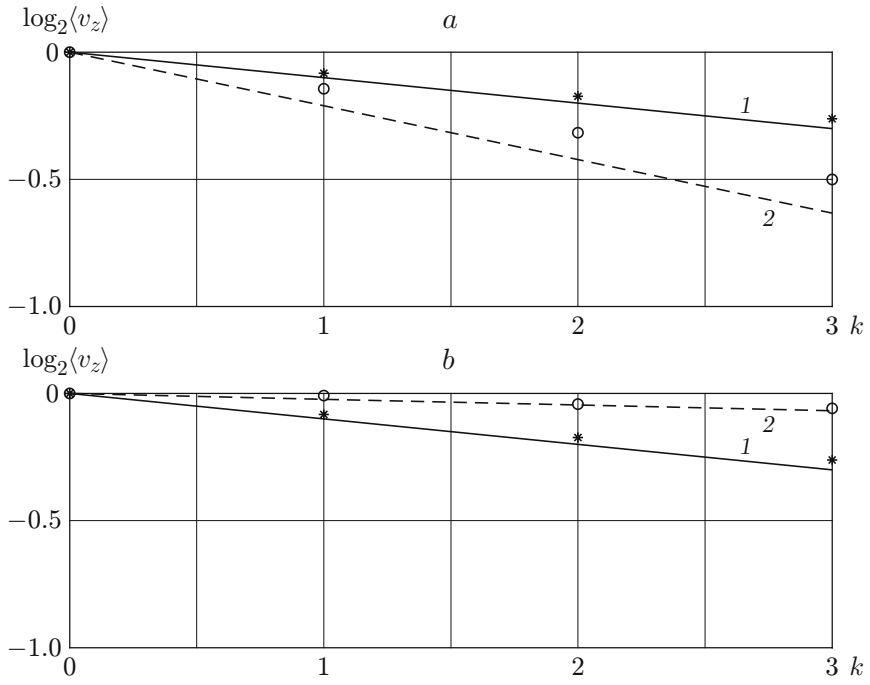

Fig. 3. Dependences of $\log_2\langle v_z\rangle$ versus the number of scales (the main flow is directed along the z axis) for $\alpha_1/\alpha_2 = 0.25$ (a) and 4 (b) (notation the same as in Fig. 2).

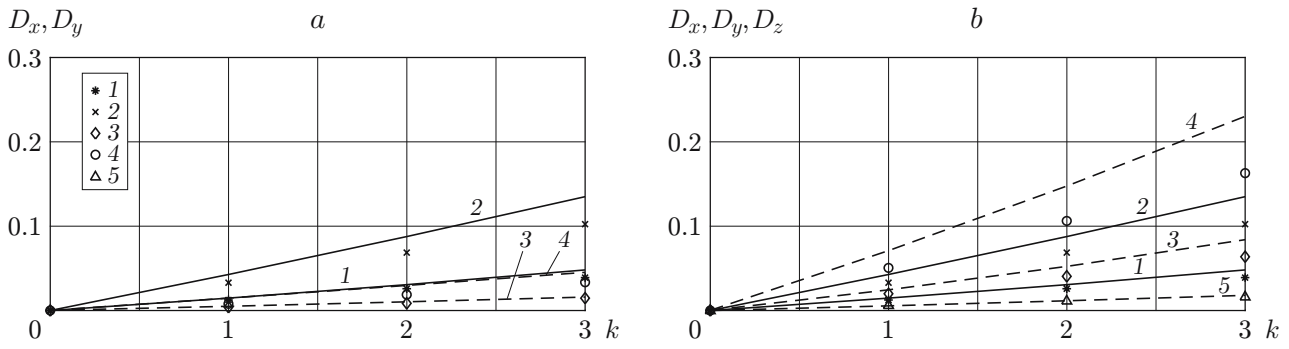

Fig. 4. Components of the variance of the field $\boldsymbol{h}$ versus number of scales (the main flow is directed along the y axis) for $\alpha_1/\alpha_2 = 0.25$ (a) and 4 (b); curves and points show the theoretical estimations and numerical calculations, respectively; curves and points 1 and 2 refer to the components D_x and D_y of the isotropic medium, respectively; curves and points 3, 4, and 5 refer to the components D_x, D_y, and D_z of the anisotropic medium, respectively.

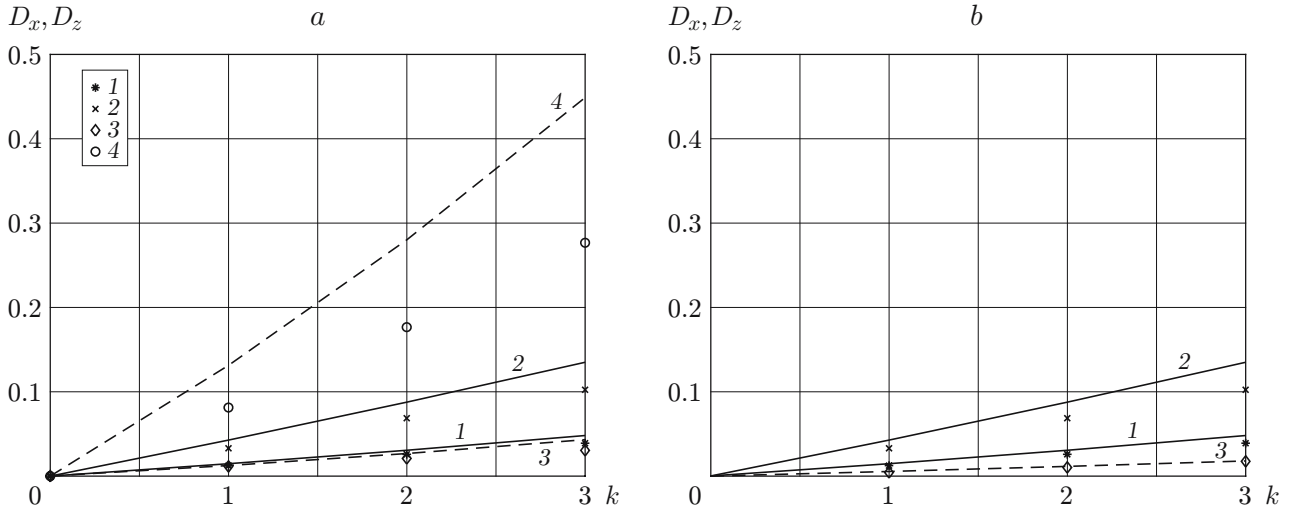

Fig. 5. Components of the variance of the field $\boldsymbol{h}$ versus number of scales (the main flow is directed along the z axis) for $\alpha_1/\alpha_2 = 0.25$ (a) and 4 (b); curves and points show the theoretical estimations and numerical calculations, respectively; curves and points 1 and 2 refer to the components D_x and D_z of the isotropic medium, respectively, and curves and points 3 and 4 refer to the components D_x and D_z of the anisotropic medium, respectively.

for anisotropic media). The estimates of the variance $\boldsymbol{h}$ are less accurate than the estimates of the mean values of the local flow in both the isotropic and anisotropic cases.

Figures 6 and 7 give curves of the variance of the local-flow field versus the number of scales taken into account for the first and second models of the medium. The quantities $\langle v_x(\boldsymbol{x})^2\rangle - \langle v_x(\boldsymbol{x})\rangle^2$, $\langle v_y(\boldsymbol{x})^2\rangle - \langle v_y(\boldsymbol{x})\rangle^2$, and $\langle v_z(\boldsymbol{x})^2\rangle - \langle v_z(\boldsymbol{x})\rangle^2$ are denoted by D'_x, D'_y, and D'_z, respectively. Figure 6a shows only two components D'_x and D'_y. In this case, $D'_z \approx D'_x$. Figure 7 gives the components D'_x and D'_z ($D'_y = D'_x$).

Conclusions. Equations were derived for the effective coefficients for the mean flow potential, mean local flow, and its variance, and the variance of the potential gradient in the stationary problem of flow in an anisotropic multifractal medium, along with power laws for the averaged components of the local flow in a self- similar medium. Theoretical results were compared with the results obtained by direct numerical modeling. From the results of the numerical experiment, it follows that the estimate of the mean local flow is fairly exact even for large values of the variance of the field. In the numerical experiments, the variance of the field $\sum_{i=-6}^{-4} \varphi(\boldsymbol{x}, \tau_i)\Delta\tau$ is equal to 0.9.

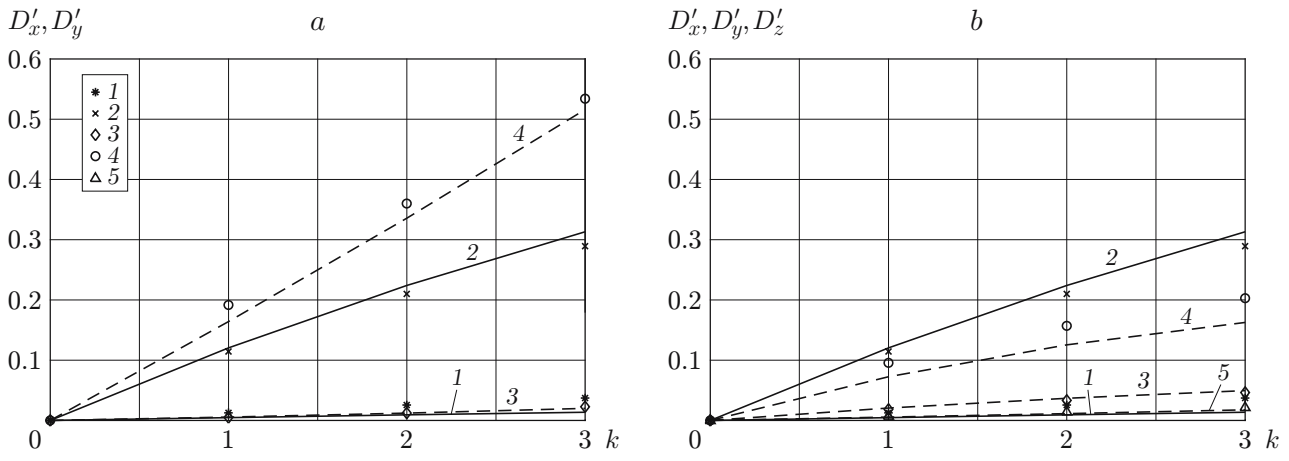

Fig. 6. Variance components of the field $\boldsymbol{v}$ versus number of scales (the main flow is directed along the y axis) for $\alpha_1/\alpha_2 = 0.25$ (a) and 4 (b): curves and points show the theoretical estimations and numerical calculations; curves and points 1 and 2 refer to the components D'_x and D'_y of the isotropic medium, respectively; curves and points 3, 4, and 5 refer to the components D'_x, D'_y, and D'_z of the anisotropic medium, respectively.

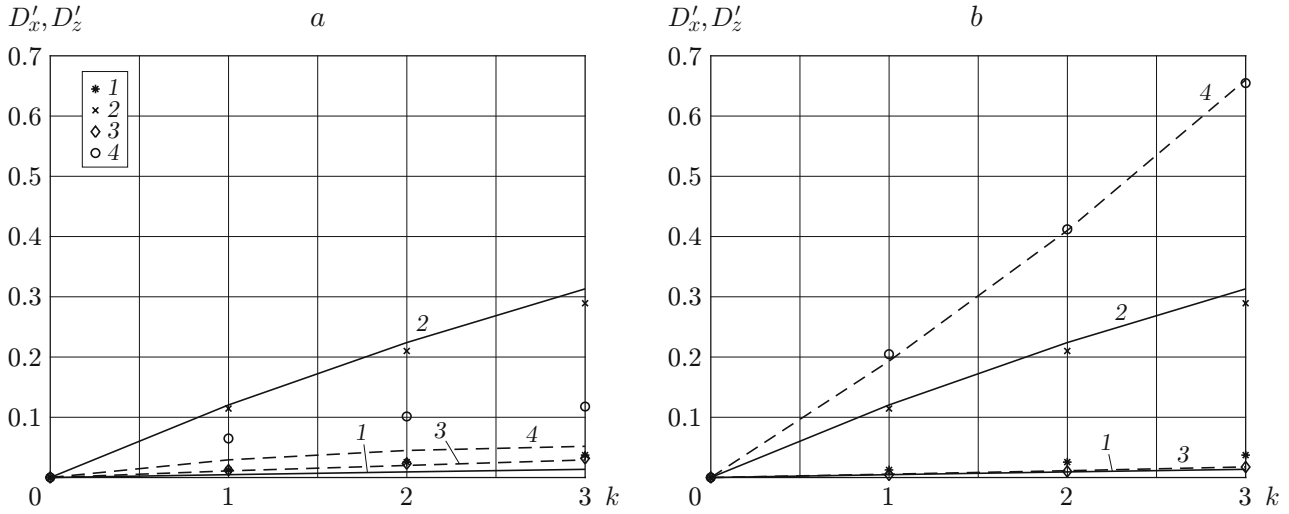

Fig. 7. Variance components of the field $\boldsymbol{v}$ versus the number of scales (the main flow is directed along the z axis) for $\alpha_1/\alpha_2 = 0.25$ (a) and 4 (b): curves and points show the theoretical estimations and numerical calculations, respectively; curves and points 1 and 2 refer to the components D'_x and D'_z of the isotropic medium, respectively; curves and points 3 and 4 refer to the components D'_x and D'_z of the anisotropic medium, respectively.

According to the experimental data given in [2, 9], for the hydraulic conductivity of sedimentary rock, the values of this variance are in the range of 0.20–0.45. For the estimated mean local flow (the plane–parallel flow is normal to a thin-layered bed (see Fig. 3a), the largest error is 8.8%. The estimate of the second statistical moments are less accurate. The estimated variances $\boldsymbol{h}$ have the largest error — 60% (see Fig. 5a). The error of the estimated variance of the local flow is 50% (see Fig. 7a). In the remaining cases, the error of the estimates is approximately 20%.

The Kolmogorov similarity hypothesis does not assume logarithmic normality and uncorrelatedness for the logarithm of the scale. Therefore, another obvious possibility of extending the above approach is to study stable distributions [12, 13] and to consider the case of conformal symmetry of conductivity. The procedure proposed in the present work allows the estimation of the effect of small-scale pulsations on the large-scale component of various fields, which is especially important if the inhomogeneity scales are in a wide range.

One of the possible applications of the results of this study is the interpretation of electromagnetic logging in oil and gas fields when the characteristic linear size of a measuring setup, for example separation or wavelength varies during measurements.

REFERENCES

1. M. I. Shvidler, *Statistical Hydrodynamics of Porous Media* [in Russian], Nedra, Moscow (1985).
2. M. Sahimi, "Flow phenomena in rocks: from continuum models, to fractals, percolation, cellular automata, and simulated annealing," *Rev. Modern Phys.*, **65**, 1393–1534 (1993).
3. U. Jackel and H. Vereecken, "Renormalization group analysis of macrovariance in directed random flow," *Water Resour. Res.*, **33**, No. 10, 2287–2299 (1997).
4. D. T. Hristopulos and G. Christakos, "Renormalization group analysis of conductivity upscaling," *Stoch. Environ. Res. Risk Assess.*, **13**, Nos. 1/2, 131–160 (1999).
5. G. A. Kuzmin and O. N. Soboleva, "Subgrid modeling of a filtration in porous self-similar media," *J. Appl. Mech. Tech. Phys.*, **43**, No. 4, 583–592 (2002).
6. A. N. Kolmogorov, "A refinement of previous hypotheses concerning the local structure of turbulence in a viscous incompressible fluid at high Reynolds number," *J. Fluid Mech.*, **13**, 82–85 (1962).
7. A. S. Monin and A. M. Yaglom, *Statistical Hydromechanics* [in Russian], Vol. 2, Nauka, Moscow (1967).
8. B. V. Gnedenko and A. N. Kolmogorov, *Limit Distributions for Sums of Independent Random Variables,* Addison-Wesley, Cambridge (1954).
9. E. A. Sudicky "A natural experiment on solute transport in a sand aquifer: Spatial variability of hydraulic conductivity and its role in the dispersion process," *Water Resources Res.*, **22**, No. 13, 2069–2082 (1986).
10. R. A. Freeze, "A random-conceptual analysis of one-dimensional ground water," *Water Resources Res.*, **43**, No. 4, 725–741 (1975).
11. V. A. Ogorodnikov and S. M. Prigarin, *Numerical Modeling of Random Processes and Fields: Algorithms and Applications*, Kluwer, Utrecht (1996).
12. D. Schertzer and S. Lovejoy, "Physical modeling and analysis of rain and clouds by anisotropic scaling multiplicative processes," *J. Geophys. Res.*, **92**, 9693–9714 (1987).
13. O. N. Soboleva, "Effective permeabilities in a porous medium log-stable statistics," *J. Appl. Mech. Tech. Phys.*, **46**, No. 6, 891–900 (2005).